Progress In Electromagnetics Research, PIER 85, 1–23, 2008

PROTOTYPE DESIGN OF COMPACT AND TUNEABLE X-BAND PRE-BUNCHED FREE ELECTRON MASER

F. Malek, J. Lucas, and Y. Huang

Department of Electrical Engineering and Electronics
The University of Liverpool
Brownlow Hill, Liverpool L69 3GJ, United Kingdom

Abstract—At the University of Liverpool, we are developing prototype free electron maser (FEM) that are compact, powerful and efficient for potential industrial applications. The design, set-up and results of a novel X-band rectangular waveguide pre-bunched free electron maser (PFEM) are presented in this paper. Our initial device operates at 10 GHz and employs two rectangular waveguide cavities (one for velocity modulation and the other for energy extraction). The electron beam used in this experiment is produced by thermionic electron gun which operates at 3 kV and up to 50 μA. The nominal beam diameter is 1 mm passing across the X-band cavity resonators. The resonant cavity consists of a thin gap section of height 1.5 mm which reduces the beam energy required for beam wave interaction. The results, progress so far and the scope of work for the next couple of months are reported.

1. INTRODUCTION

The free electron maser (FEM) is a source of microwave power which makes use of the interaction between the electron beam and electromagnetic radiation [1]. The conventional free electron laser (FEL) consists of three main components: an electron beam in vacuum, a magnetic wiggler or undulator, which stimulates the electron to emit radiation and an optical cavity formed by two mirrors, which contains and builds up the radiation. In our project, the radiation is at microwave frequencies, therefore, the mirrors will be replaced by a resonant waveguide cavity, and the term free electron maser (FEM) is used.

When an electron passes through the wiggler magnet it oscillates from side to side. The electron radiates an electromagnetic wave but at

a higher frequency than the wiggler frequency. The electron radiates almost uniformly from one end of the wiggler to the other and the resulting wave packet contains only a finite number of oscillations [2]. The wave packet has an almost square envelope. Hence its Fourier transform results to a sinc^2 intensity spectrum. This is called the spontaneous emission and is not coherent. This is because the electrons position in the beam are random, which results in random phases between the EM wave which they emit. The total radiated power is proportional to the number of electrons in the beam, i.e., the beam current, and is weak [3].

If the electrons in the beam could be bunched together to form a larger bunches separated by one period of 'optical' wave along the wiggler as they traverse it, these bunches of electrons would radiate in phase with one another. This radiation will become coherent if the electrons were tightly bunched together. The coherent radiation is sometimes called the superradiant emission [3].

The FEL mechanism which allows stimulated emission to occur requires an EM wave to interact with the electron beam. If the source of this EM wave is external, the FEM is called the FEM amplifier. Alternatively, if the spontaneous emission is allowed to build up in the waveguide resonant cavity, the source of the EM wave is the positive feedback due to the radiation from the previous electrons. This type of FEM is called the FEM oscillator. In stimulated emission, the radiated field will be much more intense that that due to spontaneous or coherent emission The stimulated emission is sometimes called the stimulated superradiant emission. The power emitted by the wiggling electron bunches is now proportional to the square of the beam current [3].

In the normal operation of conventional FEL, the process of bunching of the electron beam is essential before gain can occur and this usually means that a reasonable large electron beam current ($> 100\,\text{mA}$) is required. FEM operating at low currents will not be able to produce this natural bunching process, as the wall losses within the waveguide cavity are greater than the round-trip signal gain due to the beam-wave interaction, hence no amplification of the wave is achieved. The optical klystron method is normally used to overcome this lasing threshold (between equal gain and loss) at lower beam currents [4]. In this method, two wiggler magnets are used, separated by a dispersive section where the electron bunching process due to the first wiggler can accumulate, so that a much more efficient electron beam — EM wave interaction can obtained in the second wiggler.

The use of a pre-bunched electron beam with an FEM offers the possibility of investigating FEM physics at very low current levels of the

order of 1 to 5 mA. Doria et al have proposed a theory for the coherent emission and gain from a bunched electron beam passing through a waveguide FEM system [5]. If the electron is bunched by a klystron buncher cavity, the gain depends on the beam current and inverse square root of the input power [5]. Unfortunately, with a typical of 20 to 40 periods per wiggler, the length of this system would be large considering that the electron gun, accelerator and beam control elements have also to be accommodated.

The purpose of this research is to produce a low cost FEM mainly for industrial processing, for which the FEM offers the prospect of a microwave source with a broad tuning range, high power and reasonable efficiency which is higher than other conventional FEL or microwave devices.

At the University of Liverpool, we are developing a novel pre-bunched free electron maser (PFEM) operating at a relatively low voltage of 3 kV at a frequency of 10 GHz, using available and affordable technology. This results in a compact, powerful, efficient and low cost device potential for industrial applications, such as plasma welding torch, pollution control, microwave processing of materials and detection of shallow buried non-metallic landmine [6, 7]. The system, shown in Figure 1, consists of an input rectangular cavity (for velocity modulation of the electron beams) and an output rectangular cavity (for energy extraction). The experimental result demonstrated coherent emission and gain with a beam current of up to 50 μA.

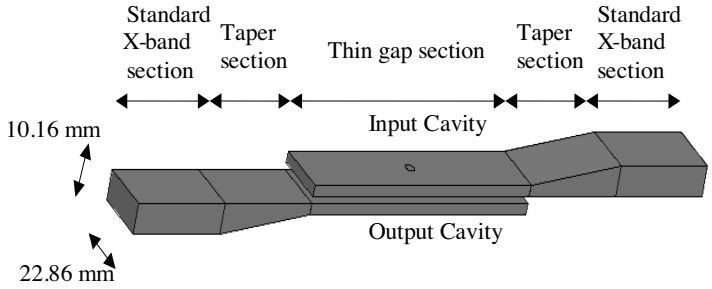

Figure 1. Diagram of PFEM showing the input cavity and output cavity.

A novel design scheme allows the PFEM to operate at a low current and accelerating voltage, maintaining a compact design. The acceleration voltage is applied directly between the electron gun filament and input cavity. The same X-band microwave source is fed into both the cavities. The phase between this output cavity and the

input cavity can be tuned by employing a phase shifter. The velocity modulated electron beam from the input cavity interacts with the microwave E-field in the output cavity, which emits strong coherent radiation, as a result, enlarged microwave power can be obtained [8, 9].

All other FEM or FEL research at universities or defence institutions either operates at very high voltage or current, or both. In all cases, the FEL cost is very expensive. The research project at Liverpool is unique because the PFEM uses low voltage and low current. Due to the low voltage, the output frequencies are in the microwave frequency range, where monitoring equipment are more readily available and cheaper. The equipment breakdowns are rare, and the ionizing (X-ray) radiation is not dangerous. Due to the low current, it is easy to maintain the high vacuum condition. Due to both (low voltage and low current), the PFEM system can be operated (powered) from the mains socket (240 Volts and 13 A).

The PFEM is tuneable, which means the operating frequency can be tuned by simply adjusting the acceleration voltage. The PFEM also requires minimal labour for design and construction. This means that the PFEM can be made at a cost cheaper than the currently available microwave source. The next sections will show a possible way forward in the design of a compact, low voltage and low current PFEM which has great potential for industrial applications.

2. PFEM DESIGN CONCEPT

The PFEM structure appears to look like a klystron, with its input cavity and output cavity, as can be seen in Figure 1. Each cavity consists of three sections: the standard X-band section, taper section and the thin gap section. The PFEM is operated in the X-band, at 10 GHz operating frequency. Hence the standard X-band section is used to interface the PFEM with other components operating in X-band region such as the E-H tuner, phase shifter, ferrite isolator, Moreno cross-coupler and X-band source.

The end of the thin gap section is terminated by a short circuit wall. The EM wave is fed into the standard X-band section of the input cavity, thus generating a standing wave TE_{10} mode wave propagation pattern in the cavity [10]. A taper section is constructed to interface between the standard X-band section and the thin gap section. In a taper section, the dimension of the waveguide varies smoothly. This allows a smooth transition of EM wave fed from the input of the standard X-band section to the thin gap section [11].

Apertures of 4 mm diameter are drilled at the centre of thin gap sections of the input cavity and output cavity respectively. An electron

gun is placed just before the input cavity. Electron beams are emitted from this electron gun source. The direction of travel of the electrons is in parallel with the TE_{10} mode field of the EM wave, ensuring strong interaction between the electron and the EM wave.

The thin gap section has a height of only 1.5 mm, and is designed to increase the intensity of the E-field strength, and also allows short electron transit time possible. This height of the thin gap section is chosen so that the transit time of electron in the thin gap section of the PFEM waveguide must be less than the time for half of a wavelength of the standing wave sinusoidal waveform.

The electrons are velocity modulated by the intense EM wave strength in the thin gap section. In other words, the electron beams are pre-bunched by the EM wave in the input cavity. At the same instance, the same EM wave fed into the input cavity from the X-band source is coupled out via a Moreno cross-coupler and coaxial cable and fed into the output cavity.

A phase shifter is placed at the output cavity, where the phase of the EM waves between the two cavities can be varied from 0 to 360 degrees. The phase in between the two cavities are varied so that, bunched electrons will arrive at the output cavity having the same phase as the EM wave, to allow synchronism with the EM wave which results in amplification of the EM wave in the output cavity.

However, the PFEM principle is different from the klystron. The klystron uses a drift space region in between the cavities, to allow the electrons to bunch. The output cavity in klystron is then located at a certain distance from the input cavity, where optimum bunching of electron occurs. The PFEM does not use the drift space region concept. In PFEM the two cavities are on top of each other, and there is no drift space (field free region) between them. A silicon 'O' ring is placed in between the two cavities for vacuum sealing purpose, and to separate the two cavities. Thin PTFE sheets are also placed in between the two cavities (in between the two thin gap sections). The separation of the two cavities in PFEM allows current flowing across the apertures of the output cavity to be monitored in the future.

PFEM uses EM wave to pre-bunch the electrons, instead of relying on drift distance as in microwave klystron. If the phase is correct between the two cavities, then the velocity modulated electron after passing the input cavity will interact with synchronism with the EM wave at the output cavity.

When the phase of the EM wave is maximum positive, i.e., peak positive amplitude, the electron will be accelerated at the fastest velocity. Due to the use of phase shifter, the electron then reaches the output cavity and encounters the EM wave that has the same phase as

the EM wave in the input cavity, i.e., peak positive amplitude. Due to the velocity modulation process in the input cavity, the electron gains velocity, $v + \Delta v$, where v is the initial velocity of the electron. In the output cavity, the electron will interact with the peak E-field positive amplitude. Energy exchange occurs where the electron beam transfers its kinetic energy into microwave energy.

When the phase of the EM wave is minimum negative, i.e., peak negative amplitude, the electron will be decelerated at the slowest velocity. Due to the use of the phase shifter, the electron then reaches the output cavity and encounters the EM wave that has the same phase as the EM wave in the input cavity, i.e., peak negative amplitude. Due to the velocity modulation process in the input cavity, the electron lost velocity, $v - \Delta v$. In the output cavity, the electron will interact with the peak E-field negative amplitude. Energy exchange occurs where the electron beam transfers its kinetic energy into microwave energy.

In the first case (positive electron velocity interacts with positive E-field), the dot product of two positives results in positive value. In the second case (negative electron velocity interacts with negative E-field), the dot product of two negatives results in a positive value. Hence, by using the phase shifter, the phase between the electrons in the input cavity is ensured to be the same as the phase of the EM wave in the output cavity. Therefore, the signs of the two elements are always the same, ensuring strong interaction between the two and microwave amplification (positive value of the dot product). This is illustrated in Figure 2.

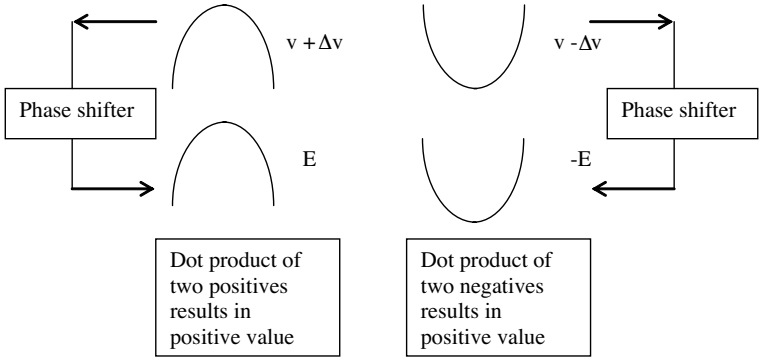

Figure 2. Illustration of interaction between the electron and EM wave, where the phase is made the same using the phase shifter.

The electron beams can be pictured as oscillating in a sinusoidal wave pattern which moves along the EM sinusoidal wave. In this sinusoidal path, some electrons are accelerated and some are

decelerated, hence a bunching process occurs. The whole mechanism is amplified as the radiation in the cavity builds up. Once the electrons are bunched, they will radiate coherently. The radiated field will be much larger than that due to spontaneous emission, because the waves from each electron are now in phase and now constructively interfere. In this case, the intensity of the coherent emission is proportional to the square of the beam current.

Hence, to achieve synchronism condition, the FEM uses the following principles, which replaces the permanent wiggler magnets used in conventional FEL and drift distance used in klystron:

(a) The electron beam is emitted just before the aperture of the input cavity to ensure its velocity component to be parallel to the direction of the TE_{10} mode of the electric field.

(b) The EM wave in the input cavity is used to bunch the electrons.

(c) The dot product **v.E** can be maintained to be positive by using a phase shifter to ensure the correct phase between the EM wave in the input cavity and the EM wave in the output cavity. Whenever **v** changes sign, due to electrons oscillatory path, **E** (in the output cavity) also changes sign.

(d) The height of the thin gap section is selected to allow short electron transit time in the gap.

The bunched beam interacting with the EM wave eliminates the need of using permanent wiggler magnets or drift distance in PFEM. Instead, higher gain can be achieved in the PFEM by using high Q factor resonant cavities. In conventional wiggler FEL, higher gain can be achieved by having larger period of permanent wiggler magnets or by adjusting the wiggler parameters.

3. PFEM DESIGN THEORY

The mathematical analysis of PFEM, with result in the derivation of the output power of the PFEM is discussed in this section. Figure 3 shows the experimental variables used for the PFEM system.

The electrons are initially accelerated through a voltage of $V_s = 3000\,\mathrm{V}$. The electron velocity is

$$v_0 = \sqrt{\frac{2eV_s}{m}} \approx \frac{c}{10} \tag{1}$$

where $\frac{e}{m}$ is the rate of electron charge to mass and c is the speed of light in vacuum.

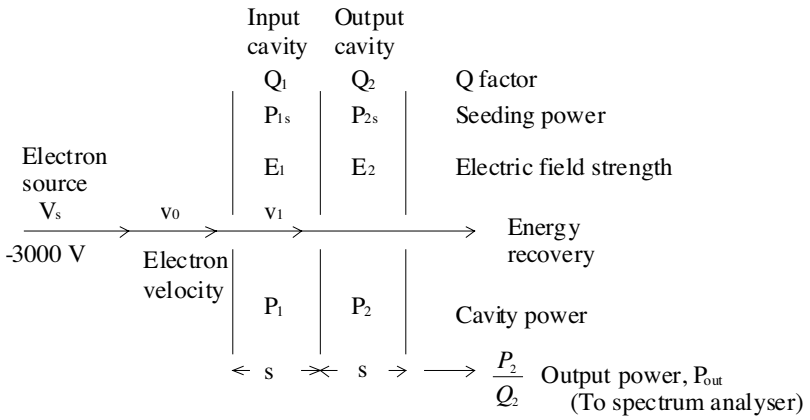

Figure 3. PFEM system variables.

While passing across the input cavity, the electron velocity (v_1) is modulated by the seeded electric field $E_1 = \frac{V_1}{s}$, with an angular frequency ω. V_1 is the small AC voltage present across the thin gap section of the input cavity. s is the length (height) of the thin gap section.

The electron velocity expression is as follows.

$$v = v_0 + v_0 \frac{1}{\pi} \frac{V_1}{V_s} \sin(\omega t) \tag{2}$$

The modulation velocity v_1, relative to v_0 is given by

$$v_1 = v_0 \frac{1}{\pi} \frac{V_1}{V_s} \sin(\omega t) \tag{3}$$

The acceleration voltage is expressed as $V_s = E_1 s = \sqrt{2 Z_0 P_1}$, and the characteristic impedance, $Z_0 = 377\,\text{Ohms}$. P_1 is the input cavity power and is related to the seeding power (P_{1s}) via the Q factor and is given by $P_1 = Q_1 P_{1s}$. The electrons then travel across the output cavity and transform kinetic energy into microwave energy. The energy change (ΔU) is obtained by multiplying the modulating factor by the voltage in the output cavity, V_2, and is given by

$$\Delta U = \frac{1}{\pi} \frac{V_1}{V_s} V_2 \tag{4}$$

where

$$V_2 = \sqrt{2 Z_0 P_2} \tag{5}$$

with P_2 being the power within the output cavity. Substitution gives

$$\Delta U = \frac{1}{\pi} \frac{\sqrt{2Z_0 P_1}\sqrt{2Z_0 P_2}}{V_s} \tag{6}$$

By substituting $Vs = 3000\,\text{Volts}$ into Equation (6), the simplified expression of ΔU is shown below.

$$\Delta U = 0.08\sqrt{P_1 P_2} \tag{7}$$

The power generated within the output cavity is $(\Delta U)I$ where I is the electron beam current. This is balanced by the power loss as indicated by the Q factor (Q_2). In other words, due to conservation of energy, the power loss by the seeded power (P_{2s}) is transferred to the output cavity (cavity power, P_2).

Hence

$$\frac{P_2}{Q_2} = 0.08\sqrt{Q_1 P_{1s} P_2} I \tag{8}$$

Squaring the LHS and RHS of the above equation gives

$$P_2 = (0.0064)\, Q_2^2 Q_1 P_{1s} I^2 \tag{9}$$

A coupler, which consists of two rectangular waveguides with coupling apertures in the common wall, is used in microwave measurements and power monitoring [12]. The output power via a cross coupler with a Q factor of Q_L is given by

$$\frac{1}{Q_2} = \frac{1}{Q_c} + \frac{1}{Q_L} \tag{10}$$

where Q_2 is the cavity Q factor, Q_L is the value of the cross coupler and Q_c is obtained directly from the spectrum analyser.

The value of the cross coupler is usually quoted in dB. For example, if the cross coupler is 10 dB, hence $\frac{1}{Q_L} = \frac{1}{10}$. If the cross coupler is 20 dB, hence $\frac{1}{Q_L} = \frac{1}{100}$ and if the cross coupler is 30 dB, hence $\frac{1}{Q_L} = \frac{1}{1000}$.

In the PFEM, it is important to have a cross coupler that extracts only a small amount of power in the cavity, in order to maintain a high Q factor in the cavity. A cross coupler value of between 20 dB and 30 dB is desirable to be used especially in the output cavity. In the input cavity, the cross coupler value is not that critical because the cross coupler is placed outside the input cavity circuit, and hence does not reduce the Q factor of the input cavity. A 24 dB Moreno cross coupler, used in previous Liverpool FEL research work is readily

available. Hence, in the PFEM system, the 24 dB cross coupler is used to be located in the output cavity. Therefore $\frac{1}{Q_L} = \frac{1}{251}$. The output power, extracted from the cavity is given by

$$P_{out} = \frac{P_2}{Q_L} \tag{11}$$

$$P_{out} = (0.0064)\,\frac{Q_2^2 Q_1}{Q_L} P_{1s} I^2 \tag{12}$$

For the input cavity, a readily available 15 dB coupler is used and placed outside the input cavity circuit.

The following parameters shown in Table 1 are used. Q_c is obtained from the spectrum analyser, Q_L is the value based on the 24 dB cross coupler used in the output cavity. Q_2 is the Q factor of the output cavity and is related to Q_c and Q_L via Equation (10). Q_1 is the Q factor for the input cavity, and is derived directly from the spectrum analyser, since the cross coupler is placed outside the input cavity circuit. P_{1s} is the seeded input power from the X-band signal generator source.

Table 1. Main parameters used in the PFEM.

Q_c	617
Q_2	178.4
Q_L	251
Q_1	893
P_{1s}	10 mWatt (10 dBm)

Based on Equation (9), the output cavity power, P_2 is shown to depend on the cavity Q factors, the seeded power and the beam current. Therefore the gain of the PFEM is proportional to the input power, P_{1s} and on the square of the beam current (I_2). The gain (in dB) is obtained when P_{1s} (in dBm) is substracted from P_2 (in dBm).

The thin gap makes a short electron transit time possible and increases the intensity of the electric field through which the electron passes. The height of this thin gap section of the waveguide, s, depends on the transit time of the electron beam in the waveguide. The transit time of an electron in the thin gap section must be less than half of the RF wavelength. Hence, the following condition must be satisfied:

$$\frac{s}{v_0} < \frac{1}{2f} \tag{13}$$

where f is the operating frequency. The chosen value of f is 10 GHz and the acceleration voltage is 3000 Volts, hence the thin gap section, s, must be less than 1.623 mm for the above condition to be satisfied. Therefore, a rounded figure of $s = 1.5$ mm is chosen in this design.

4. THE PFEM SYSTEM ARRANGEMENT

The PFEM system set-up, shown in Figure 4, consists of four main components: the electron gun, the input cavity (electron velocity modulator), the output cavity (energy extractor) and the turbo-molecular vacuum pump system. This section describes briefly these components.

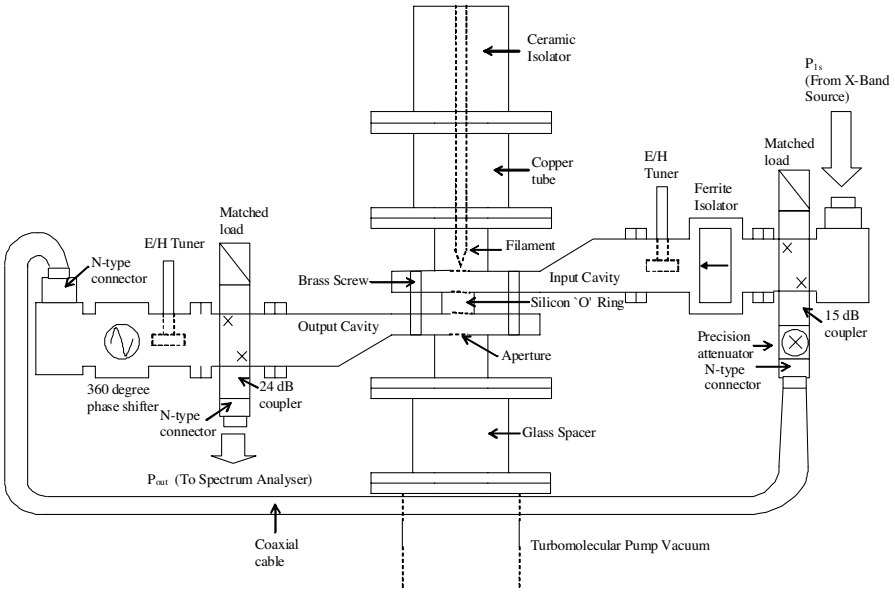

Figure 4. Diagram of Pre-Bunched Free Electron Maser (PFEM) system. The electron gun and high voltage circuits are omitted for simplicity purpose.

A simple electron gun arrangement has been used, which incorporates a cathode and an anode. The cathode is designed from tungsten filament (operated up to 50 μA). The input cavity acts as an anode. The gun is operated at voltages up to 3 kV. The supply polarity is negative [13]. The tungsten filament is powered using a VARIAC (variable auto transformer) and a step down filament transformer. The output lines of the transformer are connected to the tungsten filament.

The input cavity is placed directly below the electron gun. The output cavity is placed directly below the input cavity, separated by silicon 'O' ring for insulation purpose. This insulation is to allow the current flowing through the apertures to be measured. This input cavity is designed using a standard X-band waveguide, WR90/WG16, with internal broad dimension of 22.86 mm, and narrow dimension of 10.16 mm. As can be seen in Figure 1, each cavity consists of three main sections: the standard X-band section, the tapered section and the thin gap section.

The length of the standard X-band section is one waveguide wavelength (λ_g) which is calculated at 10 GHz for the TE_{10} mode [14, 15]. Similarly, a tapered section of one waveguide wavelength (λ_g) is placed next to this standard X-band section. In such waveguide taper, power may be lost to reflection and radiation. The taper should be designed to keep radiation reflection loss at a minimum [16]. Simulation using Vector Fields CONCERTO shows that the return loss of RF power is minimised when the taper length is designed to be equal to 1* waveguide wavelength. A thin gap section of height 1.5 mm and length 2.5∗ waveguide wavelength ($2.5 * \lambda_g$) is connected to the tapered section. Apertures of 4 mm diameter are drilled in the centre of the thin gap section to allow electrons to flow through.

The microwave power (up to 10 dBm) from the Marconi signal generator is fed into the input of the X band section of the input cavity. The same microwave power is fed into the output cavity using the 15 dB coupler, via a coaxial cable. The two cavities are fully tuned to get the best resonance by using E-H tuners, and the frequency is fixed at 10 GHz. A 360 degree phase shifter is placed at the output cavity, and this can be adjusted to ensure the correct phase between the bunched electron beams and the microwave E-field in the output cavity. Velocity modulated electron beams will flow across the apertures of the input cavity into the apertures of the output cavity. These bunched beams will strongly interact with the microwave E-field in the output cavity. At the output cavity, a 24 dB coupler is used to extract microwave signal from the cavity to the spectrum analyser. In the vacuum system, the pump is isolated from the output cavity by a glass spacer, for the purpose of current measurement flowing across the apertures of the cavities.

5. SIMULATION RESULTS

The electric field patterns for the rectangular cavity are simulated using Vector Fields CONCERTO software. The design is constructed using 2.5∗ waveguide wavelength in the thin gap section, so that 3 peaks

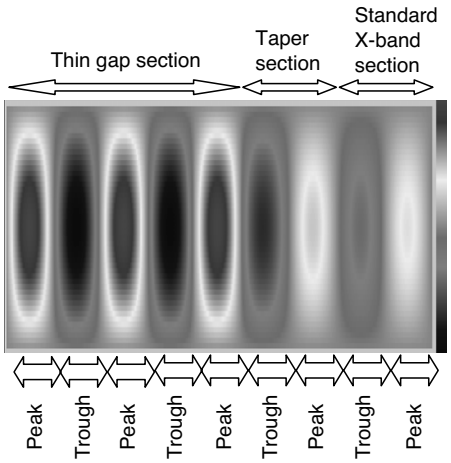

Figure 5. Thermal plot (aerial view) of electric field pattern in the PFEM system simulated using CONCERTO.

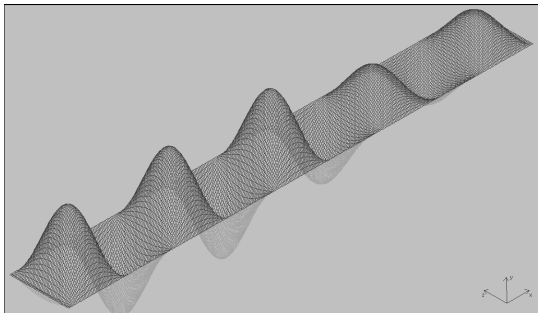

Figure 6. 3-D wave propagation plot (aerial view) of the PFEM system simulated using CONCERTO.

and 2 troughs of E-field standing waves are present in this section. Therefore the apertures can be drilled on the third peaks to allow the electrons to pass through, maintaining structure stability. The thermal plots for this design are shown in Figure 5 and Figure 7. As can be seen, the dark colours show a very strong electric field which is present in the thin gap section of the cavity. The electric field strength gradually reduces in the taper section and the standard X-band section of the cavity, i.e., the colours become lighter.

The 3-D wave propagation plots are shown in Figure 6 and Figure 8. The envelope plot of the electric field along the long length of the waveguide is shown in Figure 9. This affirms that the standing

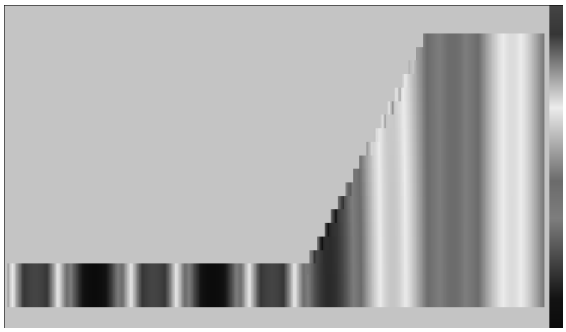

Figure 7. Thermal plot (side view) of electric field pattern in the PFEM system simulated using CONCERTO.

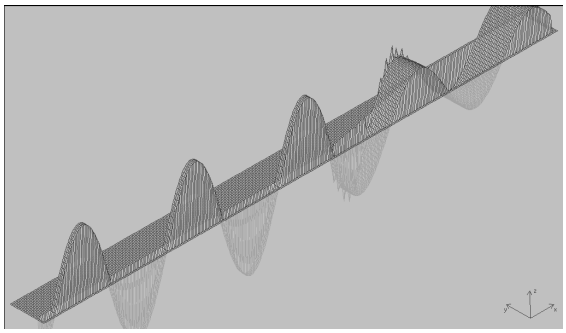

Figure 8. 3-D wave propagation plot (side view) of the PFEM system simulated using CONCERTO.

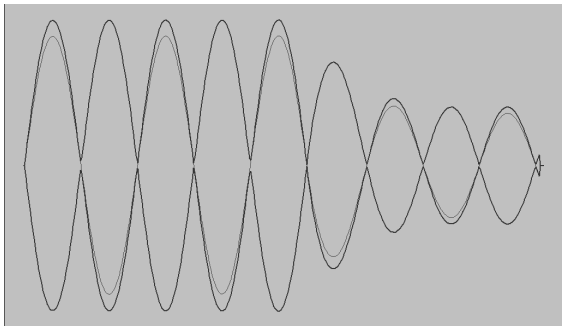

Figure 9. Envelope plot of the PFEM system simulated using CONCERTO.

wave is formed in the PFEM system, with 3 peaks and 2 troughs in the thin gap section of the system.

6. EXPERIMENTAL SET-UP

An experiment has been set-up with two stages of voltage difference. The first stage is between the filament and the input cavity. This can be called the pre-bunching stage where a low voltage (-100 V) is set up. The second stage is between the input cavity and the output cavity. This can be called the interaction stage where a high voltage (-3000 V) is set up. The correct phase between the input and output cavities is ensured using the phase shifter.

In order to realise this two stages of voltage difference, a voltage divider circuit is developed where 19 kΩ and 590 kΩ resistors are connected in series. These series resistors are then connected in parallel to the high voltage power supply (Glassman High Voltage up to 5 kV, set at negative polarity). The low voltage required for electron pre-bunching is tapped from the 19 kΩ resistor, while the high voltage required for interaction stage is tapped from the 590 kΩ resistor.

The phase shifter is placed at the output cavity, where the phase of the output cavity in relation to the input cavity can be varied between 0 to 360 degrees. The filament currents are set at 30 μA and 50 μA and 10 GHz operating frequency are chosen for both cases. It is observed that 50% of this total filament current flows across the apertures of the output cavity. The term used for this is the beam current, and hence the beam currents used in the two experiments are 15 μA and 25 μA. The output power level (dBm) reading is observed when the filament is cold. This reading is called the reference power level (dBm). The filament is heated up to the desired beam currents (15 μA or 25 μA), and the output power level (dBm) is observed. This reading is called the observed power level (dBm). The gain is the difference between the observed power level (dBm) and the reference power level (dBm).

7. RESULTS AND DISCUSSION

This gain value is observed at phases from 0 to 360 degrees, with 10 degree increments. The gain versus phase is plotted in Figures 10 and 11. These plots can be called the gain-phase curves.

Figure 10 shows the gain-phase curve at acceleration voltages of 3000 Volts, 3150 Volts and 3300 Volts, and when 15 μA beam currents are used. The gain-phase curve shows that the gain varies when phase changes from 0 to 360 degree. The curve obtained shows a sinc^2 pattern and is deduced to be caused by the electron bunches moving

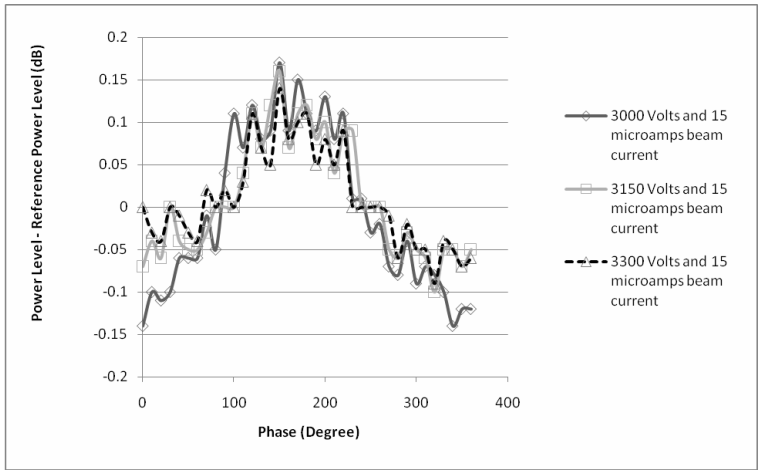

Figure 10. 3000, 3150 and 3300 Volts and 15 μA beam current.

successively in and out of phase with the EM wave as the phase is varied. It can be observed that the largest gain of 0.17 dB is achieved using 3000 Volts. At 3150 Volts, the gain is 0.16 dB, while at 3300 Volts, the gain is 0.14 dB. The same experiment is performed, but this time 25 μA beam currents are used. The result is shown in Figure 11. A gain of 0.20 dB is obtained when the voltage is 3000 Volts, 0.17 dB for 3150 Volts and 0.14 dB for 3300 Volts.

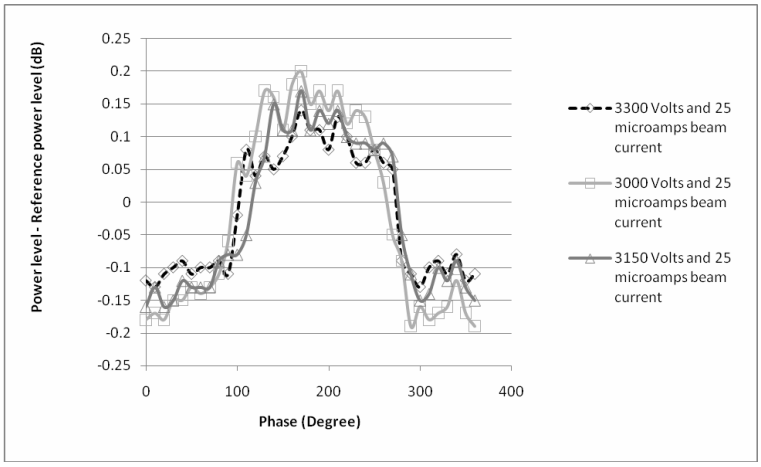

Figure 11. 3000, 3150 and 3300 Volts and 25 μA beam current.

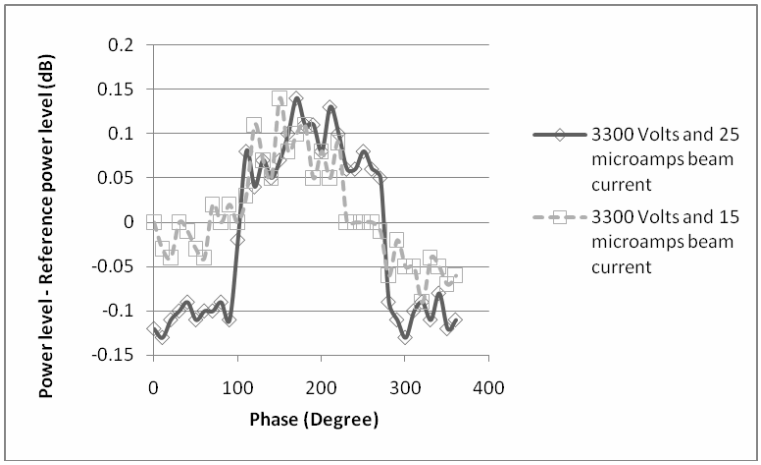

Figure 12. 3300 Volts and 25 μA and 15 μA beam current.

A comparison is now made when the beam current is changed from 15 μA to 25 μA, while maintaining the same voltage. In Figure 12, the voltage used is 3300 Volts, while 3150 Volts is used in Figure 13, and 3000 Volts is used in Figure 14. It can be observed that the phase changes by approximately 20 degree when the beam current is changed from 15 μA to 25 μA, while maintaining the voltage.

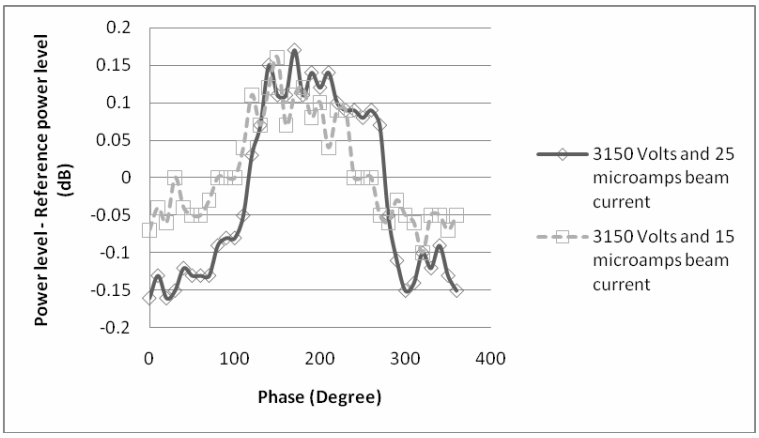

Figure 13. 3150 Volts and 25 μA and 15 μA beam current.

The result presented in this paper shows that reasonable values for gain is achieved for the power coupled out of the system, even though

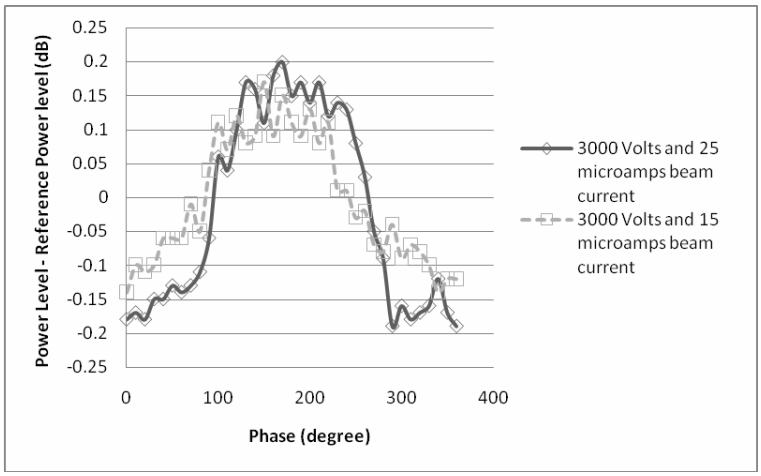

Figure 14. 3000 Volts and 25 μA and 15 μA beam current.

only 15 μA and 25 μA beam currents and low voltage are used for the electron pre-bunching. The more important result is to show that the electrons are pre-bunched in the input cavity, by having a sinc^2 shaped gain curve as the phase is varied. The EM wave is either increased or decreased after interaction with the electron beams depending on the relative phase between the two. If the phase difference is zero, the EM wave is amplified, if the phase is 180 degree, the wave is attenuated, and if the phase is 90 degree, the EM wave is not affected. A high value point on the gain curve implies that the phase of the electrons in the input cavity is the same as the phase of the EM wave in the output cavity. A low value point on the gain curve implies that the electrons in the input cavity and the EM wave in the output cavity are out of phase.

It can be seen from equation (9), that if small currents are used, (for example 50 μA or 100 μA), this results in a 'negative' gain. Positive gain values are achieved when the currents are larger than 2.345 mA. Therefore equation (9) is only valid when the current used is 2.345 mA or larger, because gain cannot be 'negative', (i.e., the output power must be more than the input power for an FEM amplifier). The experiments are performed at beam currents of 25 μA and 15 μA for the following reasons:

(a) At the initial stage, the first task is to ensure that current flows across the apertures of the output cavity. Hence, tungsten filament, which is readily available at a low cost, is used as the electron gun source.

(b) After successfully obtaining sufficient amount of beam current flows across the apertures of the output cavity, the 'real' experiment can be performed, i.e., to observe the output power or gain achieved from the system for various currents. It is decided that low currents are initially used at this stage to gain confidence in the system. The tungsten filament can be easily replaced if it burns out, as it is readily available at a low cost. If larger beam currents are to be used (2.345 mA or larger), a more powerful current source needed to be used, which is expensive to replace if it burns out.

(c) The aim from this experiment is to observe the pattern of the gain-phase curve. Although the resultant 'gain' will not be valid when using beam currents below 2.345 mA, the experiment showed that the gain-phase curve exhibits a bunching characteristic. It can be seen that the electrons are maximally bunched (in phase), and then gradually spaced apart ('un-bunched') when the phase shifter is varied gradually, until they are maximally anti-bunched (out of phase).

The gain-phase curves in Figures 10–14 are similar to the curve of the pre-bunched FEL total output power dependence on the phase delay between the bunching and the FEL input fields, in the work done by Arbel et al. [3]. Equation (9) indicates the power at the output cavity, P_2, when the electron beam is in the same phase as the EM wave. Actually, the power at the output cavity varies as the cosine of the phase angle of the electron beam as it enters the output cavity (to interact with the EM wave) [17]. Therefore, equation (9) is modified as follows.

$$P_2 = (0.0064)Q_2^2 Q_1 P_{1s} I^2 \cos(\Phi) \tag{14}$$

Where Φ is the phase angle difference between the electron beam and the EM wave in the output cavity.

The phase (degree) values on the X-axis in Figures 11–14 indicate the values on the dial of the phase shifter (10 degree resolution). It does not indicate the actual phase angle difference between the electron beam and the EM wave in the output cavity. For example, in figures 11 and 14, for the case of the voltage 3000 Volts, the maximum gain at 25 μA beam current is 0.20 dB at a phase of 170 degree. This means that when the dial of the phase shifter is at 170 degree, maximum gain occurs where the electron beam and the EM wave in the output cavity are in the same phase (phase angle difference of zero).

After showing that the electron bunches at low currents (15 μA and 25 μA), the next step is to use large beam currents (above 2.345 mA) and to observe whether the expected experimental value of

the gain matches the theory. To produce these large beam currents, a new electron gun source must be used to replace the tungsten filament. It is predicted that when high currents (above 2.345 mA) are used, the gain-phase curves will exhibit similar pattern as the gain-phase curves at small currents (15 μA and 25 μA), in Figures 10–14. For example, by using 3 mA beam current, at the peak of the curve, the expected gain value is 2.412 dB and at the minimum point of the curve, the expected gain value is −2.412 dB.

8. SUMMARY AND FUTURE WORK

The construction phase is now complete. Each of the main components has been evaluated as a separate module and testing of each component is now completed. The testing of the electron gun current emission has been performed, where the current flow across the apertures of the output cavity was measured. Results showed that around 50% of the total filament current will flow across the apertures of the output cavity.

The current design described in this paper is to apply a low voltage (−100 Volts) in between the filament and the input cavity, and a high voltage (−3000 Volts) in between the input cavity and output cavity. Over the next couple of months, a second design will be tested, where a high voltage (−3000 Volts) will be applied directly in between the filament and the input cavity.

In the future, the output power of the PFEM will be raised to Watt level for industry demonstration purpose. At the initial stage, as described in this paper, the tungsten filament was used as a source of electron. The tungsten's emission from the tip is 200 μA [10]. After gradually gaining confidence in the system, the next step is to use the Thoria coated iridium filament. Its maximum current emission is 20 mA [18]. Hence 10 mA of beam current is expected assuming 50% of the total filament current flows across the apertures of the output cavity. The use of high voltage in the electron pre-bunching stage and high current source are expected to maximise the FEM gain and output considerably.

In the subsequent step, a 'Pierce' type electron gun will be proposed for the PFEM system. The 'Pierce' type electron gun used by previous FEL researcher at Liverpool produced a maximum emission current of 285 mA [19]. Hence, with the acceleration voltage of 3 kV, and the beam current of 142 mA (assuming 50% of the 285 mA current flow across the apertures of the output cavity), the resultant cavity PFEM output power will be around 45 Watt. This value is derived from Equation (9). In addition to that if a higher output power

X-band source (23 dBm) is used in the future, this will result in a cavity PFEM output power of 0.73 KWatt, derived from Equation (9). However, emission at higher beam currents will also mean that space-charge spreading of the beam must be taken into consideration. The E-field patterns and leakages near the apertures of the thin gap sections will be simulated using the CONCERTO software. The results and analysis will be compared with the work performed by Panda [20]. The PFEM system design can be extended to higher frequencies by scaling down the waveguide dimensions appropriately or increasing the acceleration voltage. Possible applications at frequencies above 30 GHz are millimetre wave imaging, treating of tumours and high resolution radar system [21–24].

REFERENCES

1. Sabry, R. and S. K. Chaudhuri, "Formulation of emission from relativistic free electrons in a ring structure for electro-optical applications," *Progress In Electromagnetics Research*, PIER 50, 135–161, 2005.
2. Pinhasi, Y. and Y. Lurie, "Generalized theory and simulation of spontaneous and super-radiant emissions in electronic devices and free-electron lasers," *Phys. Rev.*, Vol. E65, 026501-1-8, 2002.
3. Arbel, M., A. Abramovich, A. L. Eichenbaum, A. Gover, H. Kleinman, Y. Pinhasi, and I. M. Yakover, "Superradiant and stimulated superradiant emission in a prebunched beam free-electron laser," *Phys. Rev. Lett.*, Vol. 86, 2561–2564, 2001.
4. Vinokurov, N. A., *Proceedings of the International Conference on High Energy Cherged Particle Accelerators*, Vol. 2, Serpukhov, Protvino, Russia, 1977.
5. Doria, A., R. Bartolini, J. Feinstein, G. P. Gallerano, and R. H. Pantell, "Coherent emission and gain from a bunched electron beam," *IEEE J. Quantum Electron.*, Vol. QE-29, 1428–1436, 1993.
6. Ku, H. S. and T. Yusaf, "Processing of composites using variable and fixed frequency microwave facilities," *Progress In Electromagnetics Research B*, Vol. 5, 185–205, 2008.
7. Tiwari, K. C., D. Singh, and M. K. Arora, "Development of a model for detection and estimation of depth of shallow buried non-metallic landmine at microwave X-band frequency," *Progress In Electromagnetics Research*, PIER 79, 225–250, 2008.
8. Gholami, M., "Analysis of output power delay in coaxial vircator," *Progress In Electromagnetics Research B*, Vol. 4, 1–12, 2008.

9. Li, Z., T. J. Cui, and J. F. Zhang, "TM wave coupling for high power generation and transmission in parallel-plate waveguide," *J. of Electromagn. Waves and Appl.*, Vol. 21, No. 7, 947–961, 2007.
10. Mondal, M. and A. Chakrabarty, "Resonant length calculation and radiation pattern synthesis of longitudinal slot antenna in rectangular waveguide," *Progress In Electromagnetics Research Letters*, Vol. 3, 187–195, 2008.
11. Dwari, S., A. Chakraborty, and S. Sanyal, "Analysis of linear tapered waveguide by two approaches," *Progress In Electromagnetics Research*, PIER 64, 219–238, 2006.
12. Li, Z. and T. J. Cui, "Novel waveguide directional couplers using left handed materials," *J. of Electromagn. Waves and Appl.*, Vol. 21, No. 8, 1053–1062, 2007.
13. Al-Shamma'a, A. I., A. Shaw, R. A. Stuart, and J. Lucas, "Enhancement of an electron beam buncher for a CW FEM," *Nuclear Instruments and Methods in Physics Research*, Vol. A429, 304–309, 1994.
14. Pozar, D. M., *Microwave Engineering*, John Wiley & Sons, Inc., New York, USA, 1998.
15. Ziao, J.-K., W.-S. Ji, S. Zhang, and Y. Li, "A field theoretical method for analyzing microwave cavity with arbitrary cross-section," *J. of Electromagn. Waves and Appl.*, Vol. 20, No. 4, 435–446, 2006.
16. De, A. and G. V. Attimarad, "Numerical analysis of two dimensional tapered dielectric waveguide," *Progress In Electromagnetics Research*, PIER 44, 131–142, 2004.
17. Quirk, E. G., "A pre-bunched free electron laser," Ph.D. Thesis, Department of Electrical Engineering and Electronics, The University of Liverpool, 1994.
18. Dearden, G., S. E. Mayhew, J. Lucas, and R. A. Stuart, "Spontaneous emission measurements from a low voltage pre-bunched electron beam," *Nuclear Instruments and Methods in Physics Research*, Vol. A375, 179–182, 1996.
19. Wright, C. C., "Development of a free electron maser for industrial applications," Ph.D. Thesis, Department of Electrical Engineering and Electronics, The University of Liverpool, 2000.
20. Panda, D. K. and A. Chakraborty, "Analysis of co-channel interference at waveguide joints using multiple cavity modeling technique," *Progress In Electromagnetics Research Letters*, Vol. 4, 91–98, 2008.
21. Oka, S., H. Togo, N. Kukutsu, and T. Nagatsuma, "Latest

trends in millimeter-wave imaging technology," *Progress In Electromagnetics Research Letters*, Vol. 1, 197–204, 2008.

22. Ibrahim, A. T., "Using microwave energy to treat tumors," *Progress In Electromagnetics Research B*, Vol. 1, 1–27, 2008.
23. Singh, G., "Analytical study of the interaction structure of vane-loaded gyro travelling wave tube amplifier," *Progress In Electromagnetics Research B*, Vol. 4, 41–66, 2008.
24. Mizuno, M., C. Otani, K. Kawase, Y. Kurihara, K. Shindo, Y. Ogawa, and H. Matsuki, "Monitoring the frozen state of freezing media by using millimetre waves," *J. of Electromagn. Waves and Appl.*, Vol. 20, No. 3, 341–349, 2006.